The Visibility of Features in SEM Images

© Springer Science+Business Media LLC 2018
J. Goldstein et al., *Scanning Electron Microscopy and X-Ray Microanalysis*,
https://doi.org/10.1007/978-1-4939-6676-9_8

The detection in SEM images of specimen features such as compositional differences, topography (shape, inclination, edges, etc.), and physical differences (crystal orientation, magnetic fields, electrical fields, etc.), depends on satisfying two criteria: (1) establishing the minimum conditions necessary to ensure that the contrast created by the beam–specimen interaction responding to differences in specimen features is statistically significant in the imaging signal (backscattered electrons [BSE], secondary electrons [SE], or a combination) compared to the inevitable random signal fluctuations (noise); and (2) applying appropriate signal processing and digital image processing to render the contrast information that exists in the signal visible to the observer viewing the final image display.

8.1 Signal Quality: Threshold Contrast and Threshold Current

An SEM image is constructed by addressing the beam to a specific location on the specimen for a fixed dwell time, τ, during which a number of beam electrons are injected through the focused beam footprint into the specimen. The resulting beam–specimen interactions cause the emission of BSE and SE, a fraction of which will be detected and measured with appropriate electron detectors. This measured BSE and/or SE signal is then assigned to that pixel as it is digitally stored and subsequently displayed as a gray-level image. Both the incident electron beam current and the measured BSE and/or SE signals, *Si*, involve discrete numbers of electrons: n_B, n_{BSE}, and n_{SE}. The emission of the incident beam current from the electron gun and the subsequent BSE/SE generation due to elastic and inelastic scattering in the specimen are stochastic processes; that is, the mechanisms are subject to random variations over time. Thus, repeated sampling of any imaging signal, *S*, made at the same specimen location with the same nominal beam current and dwell time will produce a range of values distributed about a mean count *n*, with the standard deviation of this distribution described by $\bar{n}^{1/2}$. This natural variation in repeated samplings of the signal *S* is termed "noise," *N*. The measure of the signal quality is termed the "signal-to-noise ratio," *S*/*N*, given by

$$\frac{S}{N} = \bar{n} / \bar{n}^{1/2} = \bar{n}^{1/2} \tag{8.1}$$

Equation (8.1) shows that as the mean number of collected signal counts increases, the signal quality *S*/*N* improves as the random fluctuations become a progressively smaller fraction of the total signal.

Figure 8.1 shows schematically the result of repeated scans over a series of pixels that cross a feature of interest. The signal value *S* changes in response to the change in the specimen property (composition, topography, etc.), but the repeated scans do not produce exactly the same response due to the inevitable noise in the signal generation processes. When an observer views a scanned image, this noise is superimposed on the legitimate changes in signal (contrast) of features in the image, reducing the visibility. Rose (1948) made an extensive study of the ability of observers viewing scanned television images to detect the contrast between objects of different size and the background in the presence of various levels of noise. Rose found that for the average observer to distinguish small objects with dimensions about 5 % of the image width against the background, the change in signal due to the contrast, ΔS, had to exceed the noise, *N*, by a factor of 5:

$$\Delta S > 5\,N \tag{8.2}$$

Synthesized digital images in Figs. 8.2 and 8.3 demonstrate how the visibility is affected by noise and the relative size of objects. Figure 8.2a shows a synthesized object from the

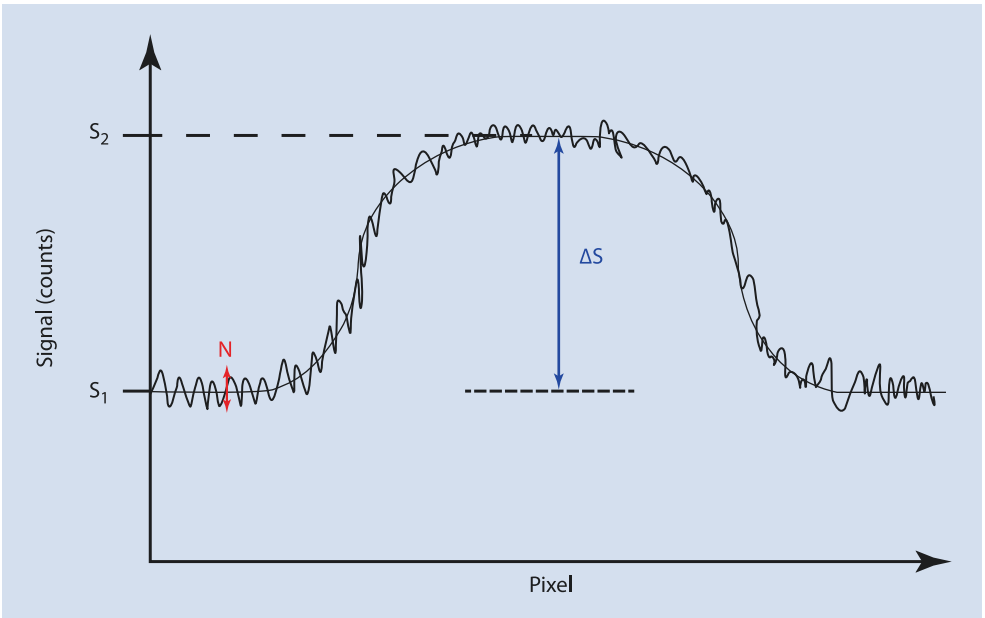

Fig. 8.1 Schematic representation of signal response across a specimen feature with the underlying long integration time average (*smooth line*)

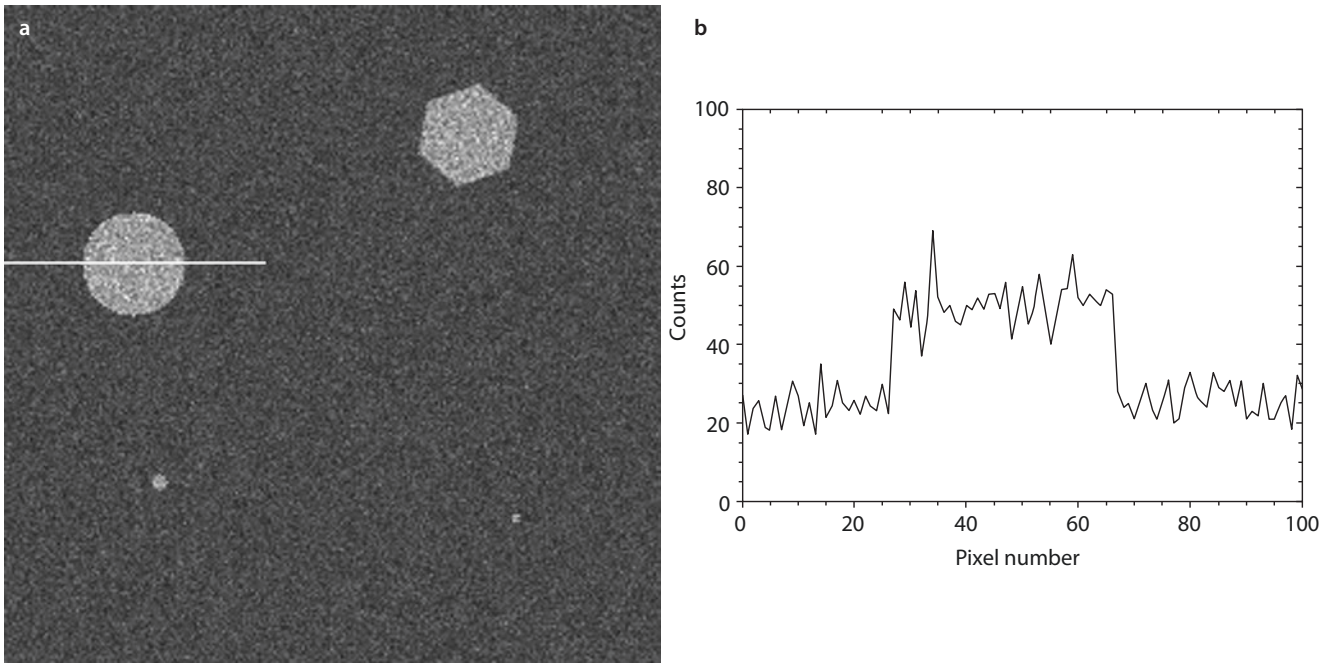

Fig. 8.2 **a** Synthesized image from the template shown in Fig. 8.3a. **b** Trace of the signal across the circular object

template shown in Fig. 8.3a with a specified signal and superimposed random noise, and Fig. 8.2b shows a plot of the signal through one of the test objects. Figure 8.3 shows synthesized images for various levels of the S and ΔS relative to N. In Fig. 8.3b $\Delta S = 5 = N$; Fig. 8.3c $\Delta S = 10 = 2N$; and Fig. 8.3d $\Delta S = 25 = 5N$, which just matches the Rose criterion. While the large-scale features are visible in all three images, the fine-scale objects are completely lost in image Fig. 8.3b, and only fully visible when the Rose criterion is satisfied in image Fig. 8.3d.

The Rose visibility criterion can be used as the basis to develop the quantitative relation between the threshold contrast, that is, the minimum level of contrast potentially visible in the signal, and the beam current. The noise can be considered in terms of the number of signal events, $N = n^{1/2}$:

$$\Delta S > 5\bar{n}^{1/2} \tag{8.3}$$

Equation (8.3) can be expressed in terms of contrast (defined as $C = \Delta S/S$) by dividing through by the signal:

$$\frac{\Delta S}{S} = C > \frac{5\bar{n}^{1/2}}{S} = \frac{5\bar{n}^{1/2}}{\bar{n}} \tag{8.4}$$

$$C > \frac{5}{\bar{n}^{1/2}} \tag{8.5}$$

$$\bar{n} > \left(\frac{5}{C}\right)^2 \tag{8.6}$$

Equation (8.6) indicates that in order to observe a specific level of contrast, C, a mean number of signal carriers, given by $(5/C)^2$, must be collected per picture element. Considering electrons as signal carriers, the number of electrons which must be collected per picture element in the dwell time, τ, can be converted into a signal current, i_s

$$i_s = \frac{\bar{n}e}{\tau} \tag{8.7}$$

where e is the electron charge (1.6×10^{-19} C). Substituting Eq. (8.6) into Eq. (8.7) gives the following result:

$$i > \frac{25e}{C^2\tau} \tag{8.8}$$

The signal current, i_s, differs from the beam current, i_B, by the fractional signal generation per incident beam electron (η for BSE and δ for SE or a combination for a detector which is simultaneously sensitive to both classes of electrons) and the efficiency with which the signal is converted to useful information for the image. This factor is given by the detective quantum efficiency (DQE) (Joy et al. 1996) and depends on the solid angle of collection and the response of the detector (see the full DQE description in the Electron Detectors module):

$$i_s = i_B(\eta,\delta)\,\mathrm{DQE} \tag{8.9}$$

Combining Eqs. (8.8) and (8.9) yields

$$i_B > \frac{25\left(1.6\times10^{-19}\ C\right)}{(\eta,\delta)\,\mathrm{DQE}\,C^2\tau} \tag{8.10}$$

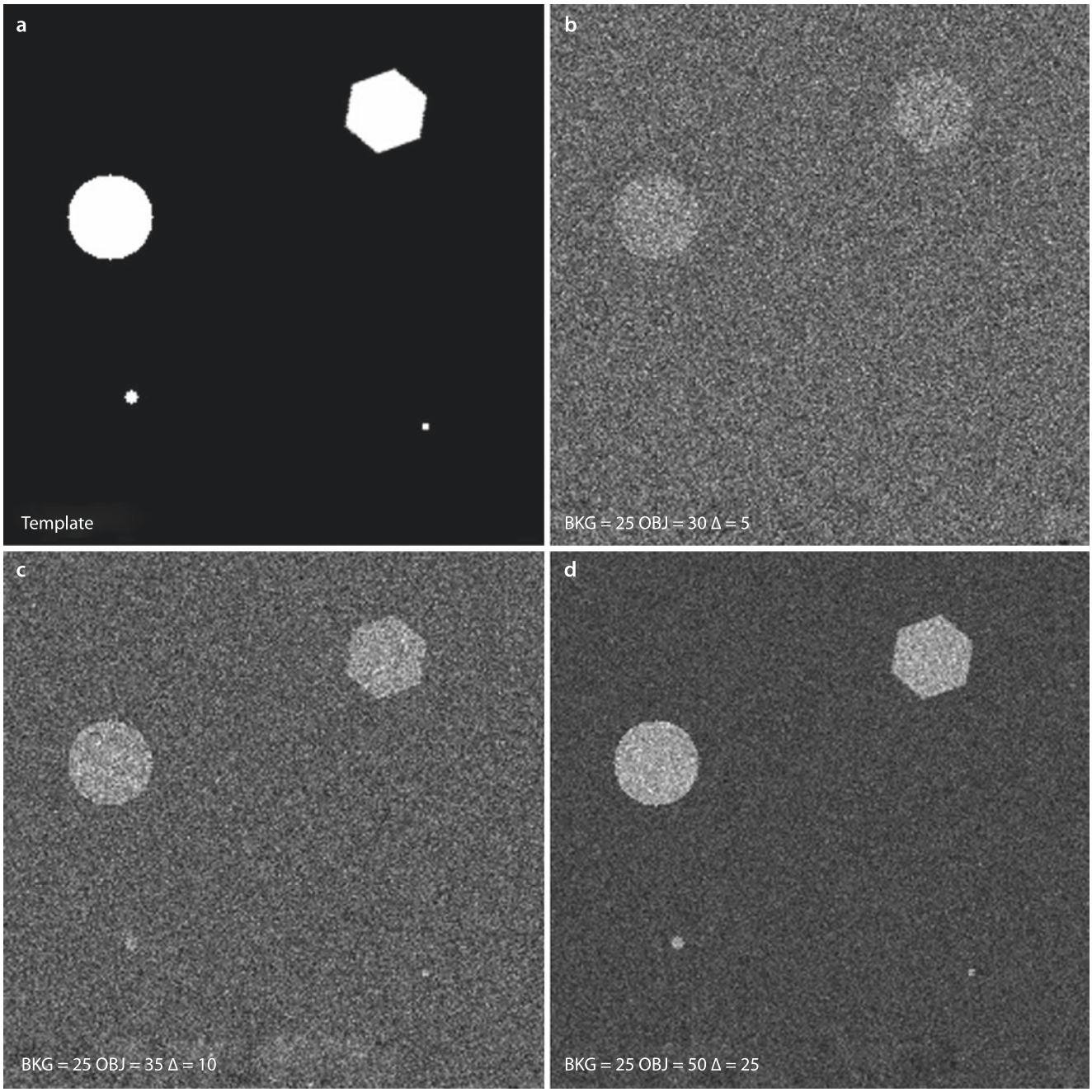

Fig. 8.3 Synthesized digital images: **a** template; **b** object $S = 5$ counts above background, $\Delta S = 5 = N$, $S/B = 1.2$; **c** object $S = 10$ counts above background, $\Delta S = 10 = 2N$, $S/B = 1.4$; **d** object $S = 25$ counts above background, $\Delta S = 25 = 5N$, $S/B = 2$

The picture element dwell time, τ, can be replaced by the time to scan a full frame, t_F, from the relation

$$\tau = \frac{t_F}{N_{\mathrm{PE}}} \tag{8.11}$$

where N_{PE} is the number of pixels in the entire image. Substituting Eq. (8.11) into Eq. (8.10),

$$i_B > \frac{\left(4\times10^{-18}\right)N_{\mathrm{PE}}}{(\eta,\delta)\,\mathrm{DQE}\,C^2 t_F}\left(\mathrm{coulomb/s = amperes}\right) \tag{8.12}$$

For an image with 1024×1024 picture elements, Eq. (8.12) can be stated as

$$i_B > \frac{\left(4\times10^{-12}\ A\right)}{(\eta,\delta)\,\mathrm{DQE}\,C^2 t_F} \tag{8.13}$$

Equation (8.12) is referred to as the "Threshold Equation" (Oatley et al. 1965; Oatley 1972) because it defines the minimum beam current, the "threshold current," necessary to observe a specified level of contrast, C, with a signal production efficiency specified by η and/or δ and the detector

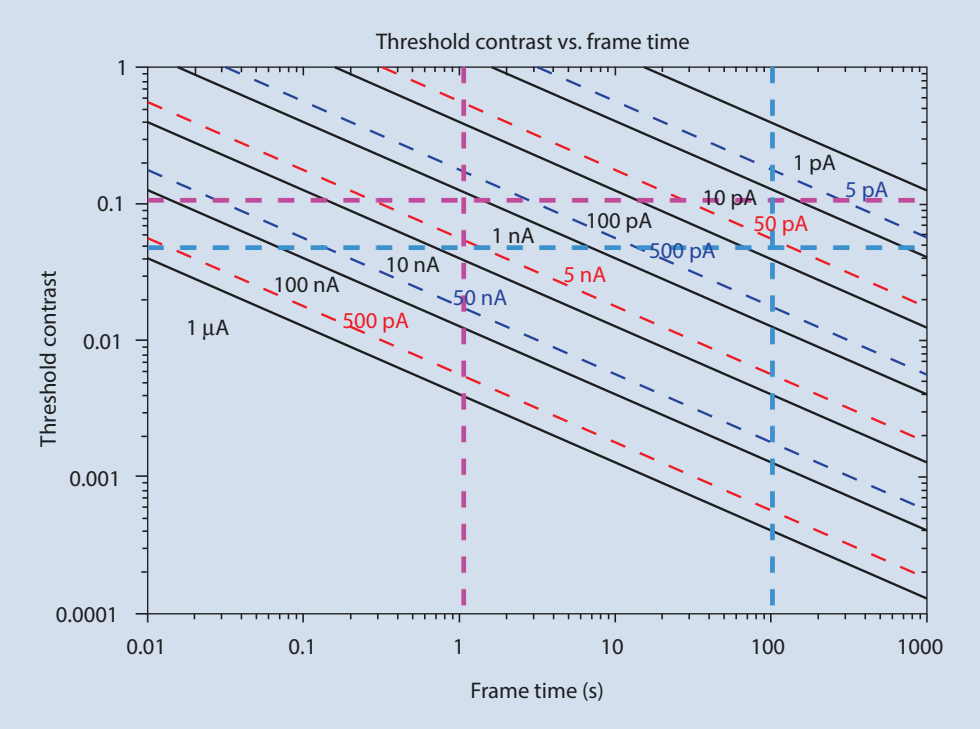

Fig. 8.4 Plot of the threshold contrast vs. frame time for an image with 1024 by 1024 pixels and an overall signal conversion efficiency of 0.25. Contours of constant current from 1 µA to 1 pA are shown

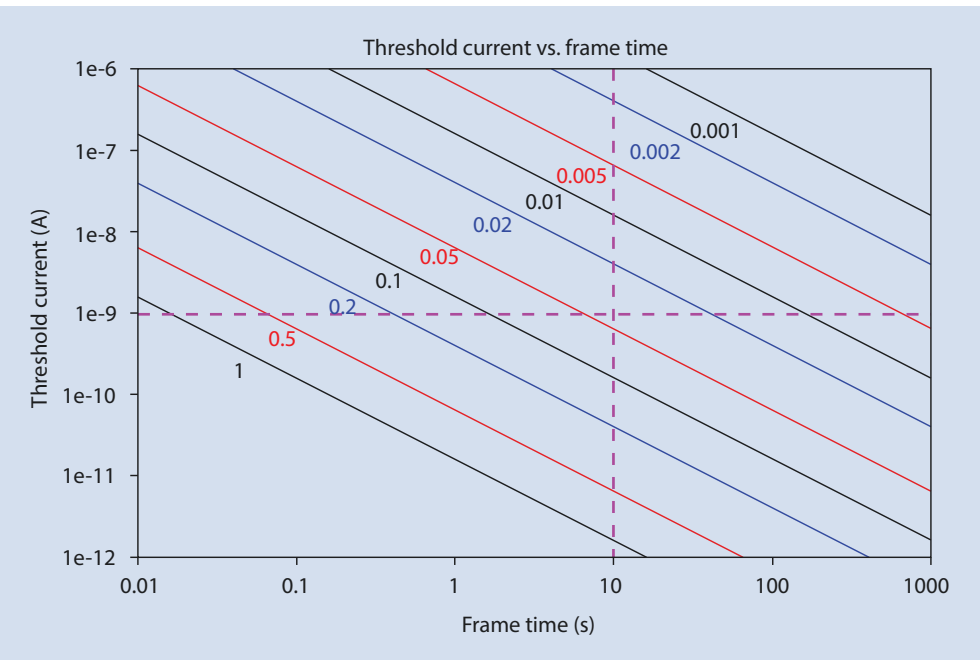

Fig. 8.5 Plot of the threshold current vs. frame time for an image with 1024 by 1024 pixels and an overall signal conversion efficiency of 0.25. Contours of constant contrast from 1 to 0.001 are shown

performance described by the DQE (Joy et al. 1996). Alternatively, if we measure the current which is available in the beam that reaches the specimen (e.g., with a Faraday cup and specimen current picoammeter), then we can calculate the minimum contrast, the so-called "threshold contrast," which can be observed in an image prepared under these conditions. Objects in the field of view that do not produce this threshold contrast cannot be distinguished from the noise of random background fluctuations. Equations (8.12 and 8.13) lead to the following *critical limitation* on SEM imaging performance:

For any particular selection of operating parameters—beam current, signal (backscattered electrons, secondary electrons, or a combination), detector performance (DQE), image pixel density and dwell time—there is always a level of contrast below which objects *cannot be detected*. Objects producing contrast below this threshold contrast cannot be recovered by applying any post-collection image-processing algorithms.

The graphical plots shown in Fig. 8.4 (threshold contrast vs. frame time for various values of the beam current) and Fig. 8.5 (threshold current vs. frame time for various values

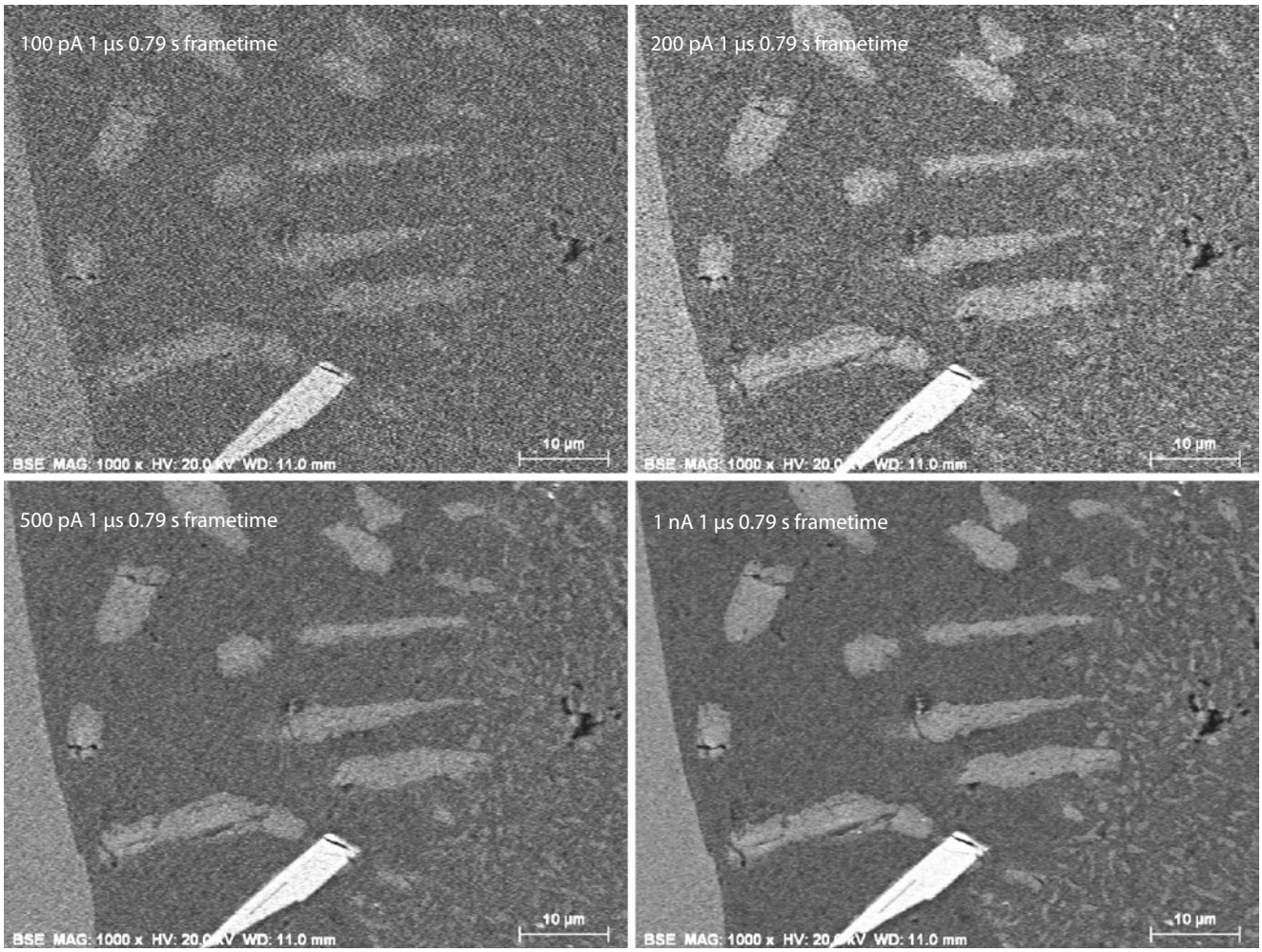

Fig. 8.6 Al-Si eutectic alloy. BSE images (1024 by 784 pixels; 1-µs pixel dwell) at various beam currents

of the contrast) provide a useful way to understand the relationships of the parameters of the Threshold Equation. These plots have been derived from Eq. (8.13) with the assumptions that the image has 1024 by 1024 pixels and the overall signal generation/collection efficiency (the product of η and/or δ and the DQE) is 0.25; that is, one signal-carrying electron (backscattered and/or secondary) is registered in the final image for every four beam electrons that strike the specimen. This collection efficiency is a reasonable assumption for a target, such as gold, which has high backscattering and secondary electron coefficients, when the electrons are detected with an efficient positively-biased E–T detector. Figure 8.4 reveals that imaging a contrast level of $C = 0.10$ (10%) with a frame time of 1 s (a pixel dwell time of ~1 µs for a 1024 × 1024-pixel scan) requires a beam current in excess of 1 nA, whereas if 100 s is used for the frame time (pixel dwell time of ~100 µs), the required beam current falls to about 10 pA. If the specimen only produces a contrast level of 0.05 (5%), a beam current above 5 nA must be used. Conversely, if a particular value of the beam current is selected, Fig. 8.5 demonstrates that there will always be a level of contrast below which objects will be effectively invisible. For example, if a beam current of 1 nA is used for a 10-s frame time, all objects producing contrast less than approximately 0.05 (5%) against the background will be lost. Once the current required to image a specific contrast level is known from the Threshold Equation, the minimum beam size that contains this current can be estimated with the Brightness Equation. A severe penalty in minimum probe size is incurred when the contrast is low because of the requirement for high beam current needed to exceed the threshold current. Moreover, this ideal beam size will be increased due to the aberrations that degrade electron optical performance.

The Rose criterion is actually a conservative estimate of visibility threshold conditions since it is appropriate for small discrete features with linear dimensions down to a few percent of the image width or small details on larger structures. For objects that constitute a large fraction of the image or which have an extended linear nature, such as an edge or a fiber, the ability of an observer's visual process to effectively combine information over many contiguous pixels actually relaxes the visibility criterion, as illustrated in the synthesized images in Fig. 8.3 (Bright et al. 1998). The effect of the size of a feature on visibility of real features can be seen in Figs. 8.6 and 8.7, which show BSE images (semiconductor detector) of a commercial aluminum–silicon eutectic casting

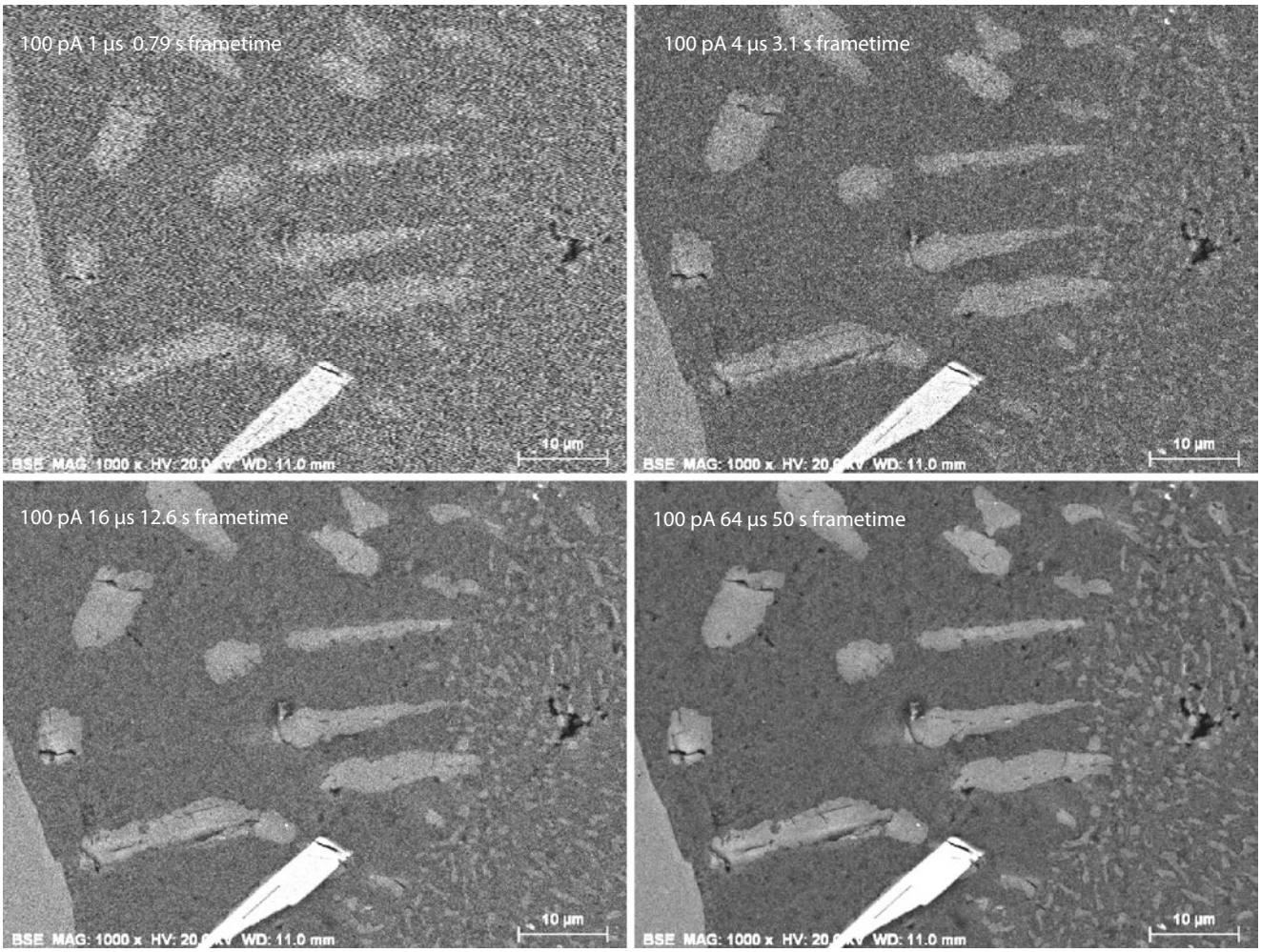

Fig. 8.7 Al-Si eutectic alloy. BSE images (1024 by 784 pixels; 100-pA beam current) pixel dwell at various frame times

alloy under various conditions. The two principal phases of this material are nearly pure Al and Si, which produce a contrast based on the respective BSE coefficients of $C = \Delta\eta/\eta_{max} = (0.14-0.13)/0.14 \approx 0.07$ or 7 % contrast. As the beam current is decreased with fixed frame time (Fig. 8.6) or the frame time is decreased with fixed beam current (Fig. 8.7), the visibility of the fine-scale features at the right-hand side of the image diminishes and these small features are eventually lost, whereas the large-scale features on the left-hand side of the image remain visible over the range of experimental parameters despite having the same compositional difference and thus producing the same contrast.

While the Threshold Equation provides "gray numbers" for the threshold parameters due to the variability of the human observer and the relative size of objects, the impact of the Threshold Equation must be considered in developing imaging strategy. Unfortunately, poor imaging strategy can render the SEM completely ineffective in detecting the features of interest. A careful imaging strategy will first estimate the likely level of contrast from the objects of interest (or assume the worst possible case that the features being sought produce very low contrast, e.g., <0.01) and then select instrument parameters capable of detecting that contrast. An example is shown in Fig. 8.8, which shows a sequence of images of a polished carbon planchet upon which a droplet containing a dilute salt was deposited by inkjet printing. The images were prepared at constant beam current but with increasing pixel dwell time, which represents a section through the Threshold Equation plot shown in Fig. 8.9. Even the largest-scale features are lost in the image prepared with the shortest dwell time. Careful study of these images reveals that new information is being added throughout the image sequence, and likely there would be additional information recovered with further increases in the pixel time or by increasing the beam current.

Finally, it must be recognized that there is a substantial "observer effect" for objects producing contrast near the threshold of visibility: different observers may have substantially different success in detecting features in images (Bright et al. 1998). Thus the threshold current or threshold contrast calculated with Eq. (8.12) should be considered a "fuzzy number" rather than an absolute threshold, since visibility depends on several factors, including the size and shape of the features of interest as well as the visual acuity of the particular observer and his/her experience in evaluating images. The limitations imposed by the threshold equation and the

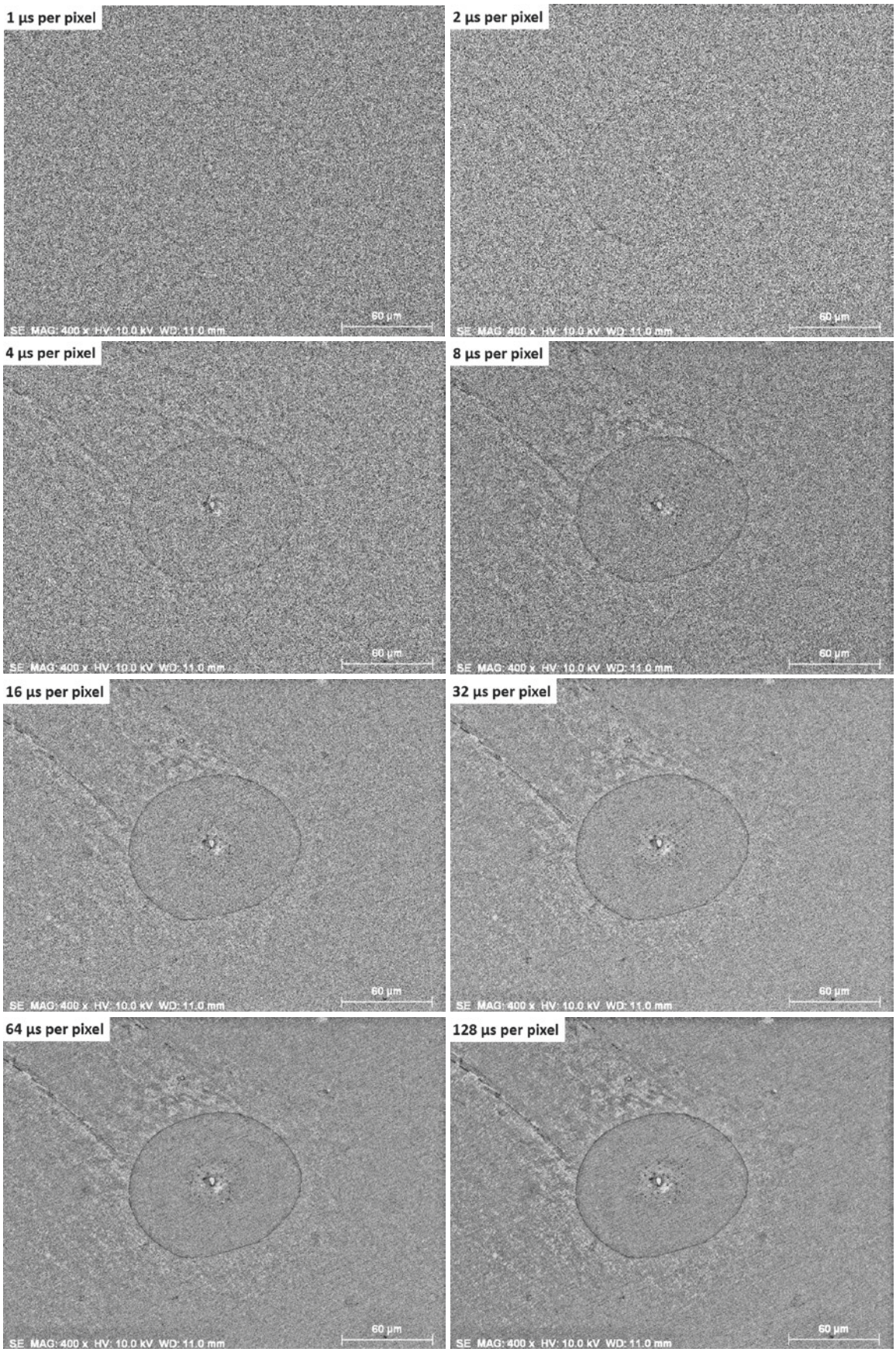

Fig. 8.8 Threshold imaging visibility; image sequence with increasing pixel dwell time at constant beam current. Inkjet deposited droplet on carbon planchet; $E_0 = 10$ keV; Everhart–Thornley (positive bias) detector. Post-collection processing with ImageJ (FIJI) CLAHE function

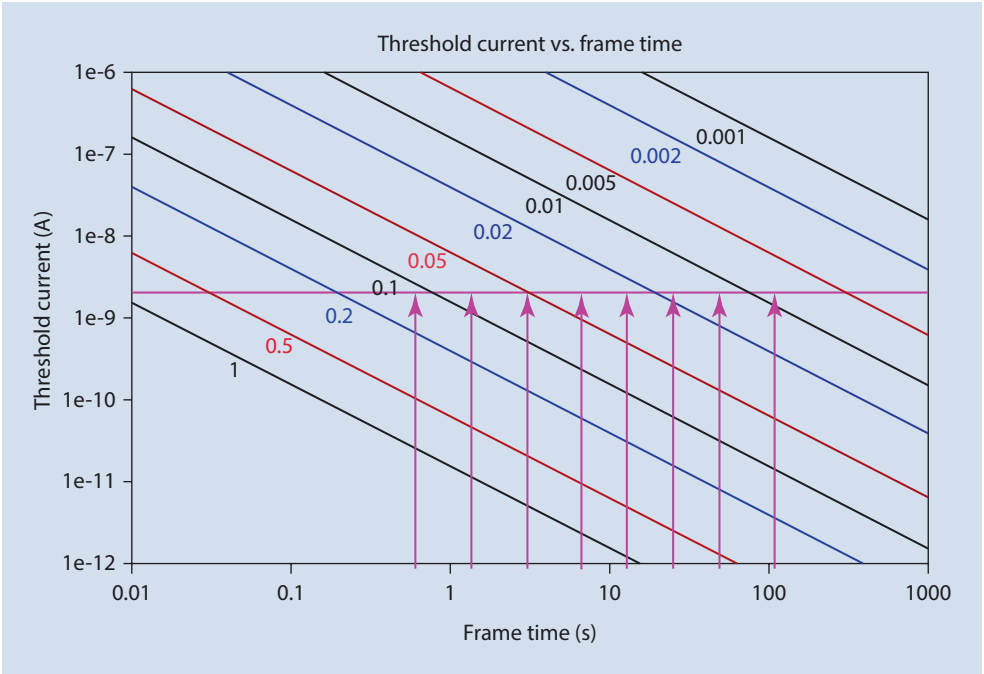

Fig. 8.9 Threshold current plot showing time sequence at constant beam current. Contours of constant contrast from 1 to 0.001 are shown

observer effect mean that a negative result in an SEM study, that is, the failure to find an expected feature in an image, may occur because of the choice of imaging conditions and the observer's limitations, not because the feature does not exist in the specimen under study. Thus, best practices in SEM imaging of low contrast features must include a comprehensive strategy to systematically vary the imaging parameters, including beam current and dwell time, to be sure that the visibility threshold is adequately exceeded before an object can be declared to be absent with a high degree of confidence.

References

Bright DS, Newbury DE, Steel EB (1998) Visibility of objects in computer simulations of noisy micrographs. J Micros 189:25–42

Joy DC, Joy CS, Bunn RD (1996) Experimental measurements of the efficiency, and the static and dynamic response of electron detectors in the scanning electron microscope. Scanning 18:181

Oatley CW (1972) The scanning electron microscope: Part 1 the instrument. Cambridge University Press, Cambridge

Oatley CW, Nixon WC, Pease RFW (1965) Scanning electron microscopy. In: Advances in electronics and electron physics. Academic Press, New York, p 181

Rose A (1948) Television pickup tubes and the problem of vision. In: Marton L (ed) Advances in electronics and electron physics, vol 1. Academic Press, New York, p 131